

Biophysical Journal, Volume 111

Supplemental Information

Are Filopodia Privileged Signaling Structures in Migrating Cells?

Heath E. Johnson and Jason M. Haugh

Supplementary Material

Are filopodia privileged signaling structures in migrating cells?

by Heath E. Johnson and Jason M. Haugh

Text S1: Methods supplement

Derivation of filopodial fluorescence, membrane marker (Eq. 4)

We first consider a uniformly distributed membrane marker with area density M . Referring to the geometry illustrated in Fig. 1A, we adopt polar coordinates (r, θ) , with $\theta = 0$ pointed in the +z-direction, and hence we express z as follows.

$$z = h + R + r \cos \theta$$

The total background-subtracted fluorescence ‘volume’ of the filopod, given by $f_f A_f$, is calculated by integrating over the volume of the cylinder, weighting by $e^{-z/d}$ as shown in Eq. 1 of the main text. Since the fluorophore is confined to the boundary at $r = R$, we invoke the Dirac delta function, $\delta(x)$, and express the integral as follows.

$$\begin{aligned} f_f A_f &= \alpha M \left[2 \int_0^R \int_0^\pi \delta(r - R) e^{-(h+R+r \cos \theta)/d} r dr d\theta \right] L \\ &= 2\alpha e^{-(h+R)/d} M R L \int_0^\pi e^{-R \cos \theta / d} d\theta \end{aligned}$$

The fluorescence intensity at the center of the cell is simply

$$\begin{aligned} f_c &= \alpha M \int_0^\infty \delta(z - h) e^{-z/d} dz \\ &= \alpha e^{-h/d} M \end{aligned}$$

And so the expression for Φ as defined in the main text is found.

$$\Phi = \frac{f_f A_f}{f_c d L} = 2\rho e^{-\rho} \int_0^\pi e^{-\rho \cos \theta} d\theta; \quad \rho = \frac{R}{d}$$

Finally, an integral identity for $I_0(x)$, a modified Bessel function of the first kind, is applied.

$$I_0(x) = \frac{1}{\pi} \int_0^\pi e^{x \cos \theta} d\theta = \frac{1}{\pi} \int_0^\pi e^{-x \cos \theta} d\theta$$

This yields the expression for Φ_{mem} given as Eq. 4 in the main text.

Derivation of filopodial fluorescence, volume marker (Eq. 5)

Following the same approach as above, now for a uniformly distributed volume marker with concentration $[F]$, we obtain the following. Note that the constant void fraction ε_f has been assumed for the filopod.

$$\begin{aligned} f_f A_f &= \alpha \varepsilon_f [F] \left[2 \int_0^R \int_0^\pi e^{-(h+R+r \cos \theta)/d} r dr d\theta \right] L \\ &= 2\alpha e^{-(h+R)/d} \varepsilon_f [F] L \int_0^R \int_0^\pi e^{-r \cos \theta / d} r dr d\theta; \\ f_c &= \alpha e^{-h/d} [F] d; \\ \Phi &= \frac{2\varepsilon_f e^{-\rho}}{d^2} \int_0^R \int_0^\pi e^{-r \cos \theta / d} r dr d\theta \end{aligned}$$

Invoking the properties of Bessel functions, the above is evaluated as follows.

$$\begin{aligned}\Phi &= \frac{2\pi\epsilon_f e^{-\rho}}{d^2} \int_0^R I_0(r/d) r dr \\ &= 2\pi\epsilon_f e^{-\rho} \rho I_1(\rho)\end{aligned}$$

This is equivalent to the expression for Φ_{cyt} given as Eq. 5 in the main text.

Derivation of filopodial fluorescence, translocation biosensor (Eq. 6)

For a translocation biosensor, with average free concentration $[B]_f$ and average membrane-bound density C_f in the filopod, we apply the same approach and results from above to calculate total fluorescence.

$$\begin{aligned}f_f A_f &= 2\alpha e^{-(h+R)/d} L \left(\epsilon_f [B]_f \int_0^R \int_0^\pi e^{-r \cos \theta / d} r dr d\theta + C_f R \int_0^\pi e^{-R \cos \theta / d} d\theta \right) \\ &= 2\pi\alpha e^{-(h+R)/d} L \left(\epsilon_f [B]_f d^2 \rho I_1(\rho) + C_f R I_0(\rho) \right) \\ &= \alpha e^{-h/d} L d \left(d [B]_f \Phi_{\text{cyt}} + C_f \Phi_{\text{mem}} \right)\end{aligned}$$

Invoking Eq. 2 for the fluorescence intensity at the cell center, f_c , and combining with the above yields the expression for Φ given as Eq. 6 in the main text.

Specification of d values for various excitation wavelengths

The characteristic penetration depth (d) of an evanescent wave can be estimated from the excitation wavelength ($\lambda = 442$ nm for TFP, 561 nm for tdTomato and mCherry), the angle of incidence of the beam ($\theta_i \approx 70^\circ$), and the refractive indices of glass ($n_1 = 1.52$) and aqueous solutions ($n_2 = 1.33$) as follows.

$$d = \frac{\lambda}{4\pi(n_1^2 \sin^2 \theta_i - n_2^2)^{1/2}}$$

Thus, d values of 68 nm and 86 nm were calculated for TFP and tdTomato/mCherry, respectively.

Image acquisition and processing

Live-cell imaging by TIRF microscopy and image processing were performed as described previously (1), and additional details are provided here. The XY optical resolution is set by the pixel side length of 256 nm (based on the pixel density of the camera and the overall magnification). Supplementary Figure S1 illustrates the image analysis workflow for a representative cell, starting with a raw image among many in a stack of sequential images (Fig. S1A). The filopodia and (non-filopodial) cell region were identified as described previously, and the center region of the cell was determined. In brief, filopodia were identified using a tophat filter applied to the binary cell mask, healing discontinuities and removing structures smaller than 15 pixels. The center region was then determined by subtracting filopodia masks from the cell mask and eroding it further by a 2.5 μm diameter disk (Fig. S1B). The filopodia were tracked across sequential images as described previously (1).

For the analysis presented in this paper, the region associated with each filopod in each image was determined by dilating the filopod mask in the TFP channel (Fig. S1C). This

step is important because it ensures that all of the filopod's fluorescence is captured, and because there is a slight focal difference between wavelengths. The area A_f associated with each filopod region (in nm^2 , based on the square of the pixel side length) and the mean background-subtracted intensity of that region, f_f , were determined. Note that the background fluorescence is already subtracted, so the value of the total fluorescence, $f_f A_f$, is not sensitive to the degree of dilation. Finally, the length of each filopod, L , was estimated as the major axis of an ellipse drawn around the filopod region (without dilation). This quantity was expressed in units of nm according to the pixel side length as described above. These quantities, together with the appropriate value of d and the mean background-subtracted intensity of the center region, f_c , were used to calculate Φ for each fluorescent protein and filopod (Eq. 3). This quantity was averaged over the duration of the filopod across multiple frames (if applicable). To reduce noise, frames in which filopodia with a mean GPI or Akt-PH intensity less than 20% of the center region intensity were excluded. All calculations were executed using MATLAB (MathWorks).

Estimation of filopod radius from Φ_{mem} or Φ_{cyt} value

For cells expressing the membrane marker GPI-tdTomato, the value of Φ_{mem} for each filopod was determined from the data, and the corresponding values of ρ (Eq. 4, main text) was identified by iterative root finding. By multiplying the estimated ρ by $d = 86$ nm for 561-nm excitation, the estimated radius R was found. This value of R was converted back to dimensionless ρ for the TFP channel by dividing by $d = 86$ nm for 442-nm excitation, and then comparison of the measured Φ_{cyt} for TFP and Eq. 5 of the main text yielded an estimate of the void fraction, ε_f , for each filopod. For the cells co-expressing mCherry-AktPH and TFP, the Φ_{cyt} for TFP was determined from the data as before, and Eq. 5 of the main text was used to estimate ρ (by iterative root finding), assuming a nominal value of $\varepsilon_f = 0.62$. By multiplying the estimated ρ by $d = 68$ nm for 442-nm excitation, the estimated radius R was found. All calculations were executed using MATLAB (MathWorks).

Specification of the contact area region adjacent to a filopod

In each applicable frame, a circle with radius $5.12 \mu\text{m}$ (corresponding to 20 pixel side-lengths), centered at the base of the filopod, was drawn. Within this circle, the non-filopodial region of the cell was identified (Fig. S1D). Prior to this, pixels that are part of the low intensity cell edge were excluded by eroding the cell mask by a 5-pixel radius disk. All operations were executed using MATLAB (MathWorks).

Calculation of adjusted intensity of the adjacent region

We used the TFP data to estimate a void fraction for the adjacent region, ε_a , relative to the center. This was taken as the ratio of the TFP intensity in the adjacent region divided by that of the center region. Then, turning to the mCherry-AktPH data, the ratio of the intensity of the adjacent region, f_a , to that of the center region (incorporating Eq. 2 from the main text) is as follows.

$$\frac{f_a}{f_c} = \frac{d\varepsilon_a[B]_a + C_a}{d[B]_c + C_c}$$

Incorporating the same assumptions as in the derivation of Eqs. 7 & 8 in the main text, we obtain

$$\frac{f_a}{f_c} = \varepsilon_a + \frac{T_a}{dK_D}$$

With f_a/f_c taken from the AktPH data and ε_a estimated from the TFP data, the ratio T_a/dK_D was estimated for each adjacent region. Hence, the adjusted fluorescence of the adjacent region was calculated as follows.

$$f_{a,adjusted} = f_c \left(1 + \frac{T_a}{dK_D} \right)$$

It suffices to compare the quantities $1+T_f/dK_D$ and $1+T_a/dK_D$ as shown in Fig. 3D of the paper. All calculations were executed using MATLAB (MathWorks).

Classification of filopodia as associated with protruding, retracting, or stationary regions

To classify cell regions based on their motility status, we calculated the relative protrusion and retraction on an angular basis about the cell centroid using overlap of cell masks between frames as described previously (2). This data was then used to generate a kymograph-like map of membrane protrusion/retraction as a function of time and angular position relative to the centroid. An averaging filter was applied to this “map” in space and time to capture only the bulk protrusion and retraction events. This smoothed protrusion/retraction map was then segmented into 3 bins using k-means clustering (Fig. S2A). The highest bin was marked as protruding, the middle one as stationary, and the bottom one as retracting. The filopodia locations were also binned with respect to angle relative to the cell centroid, and the associated motility status of the bin for each filopod in each image was determined. Finally, each filopod was classified by whichever motility status was most frequent during the filopod lifetime.

References

1. Johnson, H. E., S. J. King, S. B. Asokan, J. D. Rotty, J. E. Bear, and J. M. Haugh. 2015. F-actin bundles direct the initiation and orientation of lamellipodia through adhesion-based signaling. *J Cell Biol* 208:443-455.
2. Welf, E. S., S. Ahmed, H. E. Johnson, A. T. Melvin, and J. M. Haugh. 2012. Migrating fibroblasts reorient directionality by a metastable, PI3K-dependent mechanism. *J. Cell Biol.* 197:105-114.

Supplementary Figures

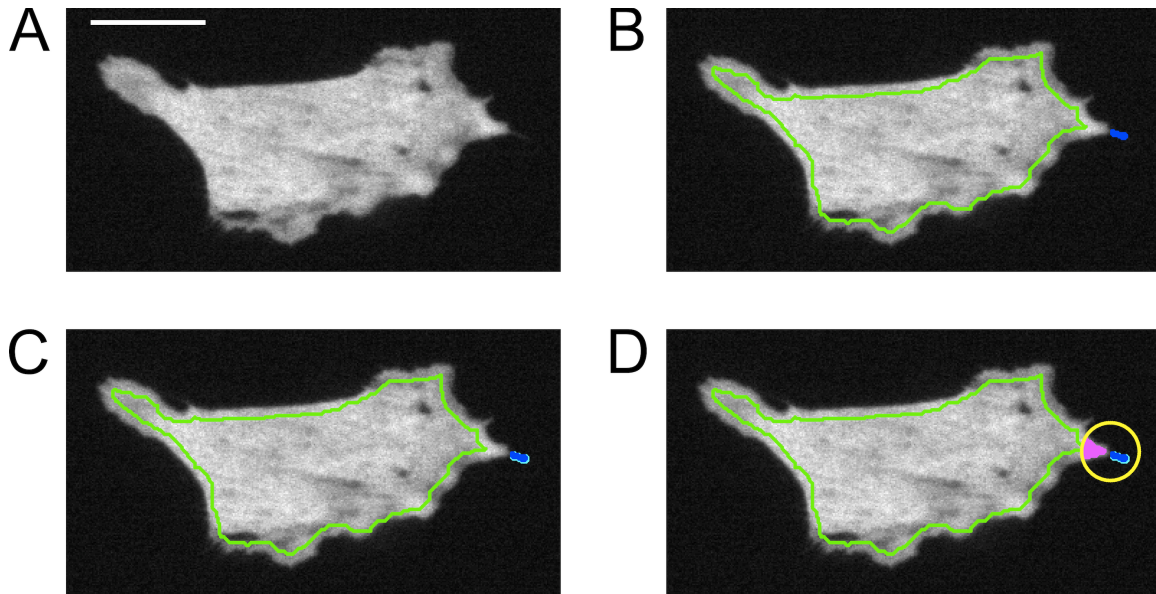


Figure S1. Identification of regions in TIRF images. *a)* TIRF image showing an entire cell expressing the volume marker, TFP. Scale bar = 20 μm . *b)* Demarcation of a filopod region (filled in blue) and the cell's center region (outlined in green). *c)* Dilation of the filopod region (extra area colored cyan). *d)* Identification of the adjacent area (filled in magenta).

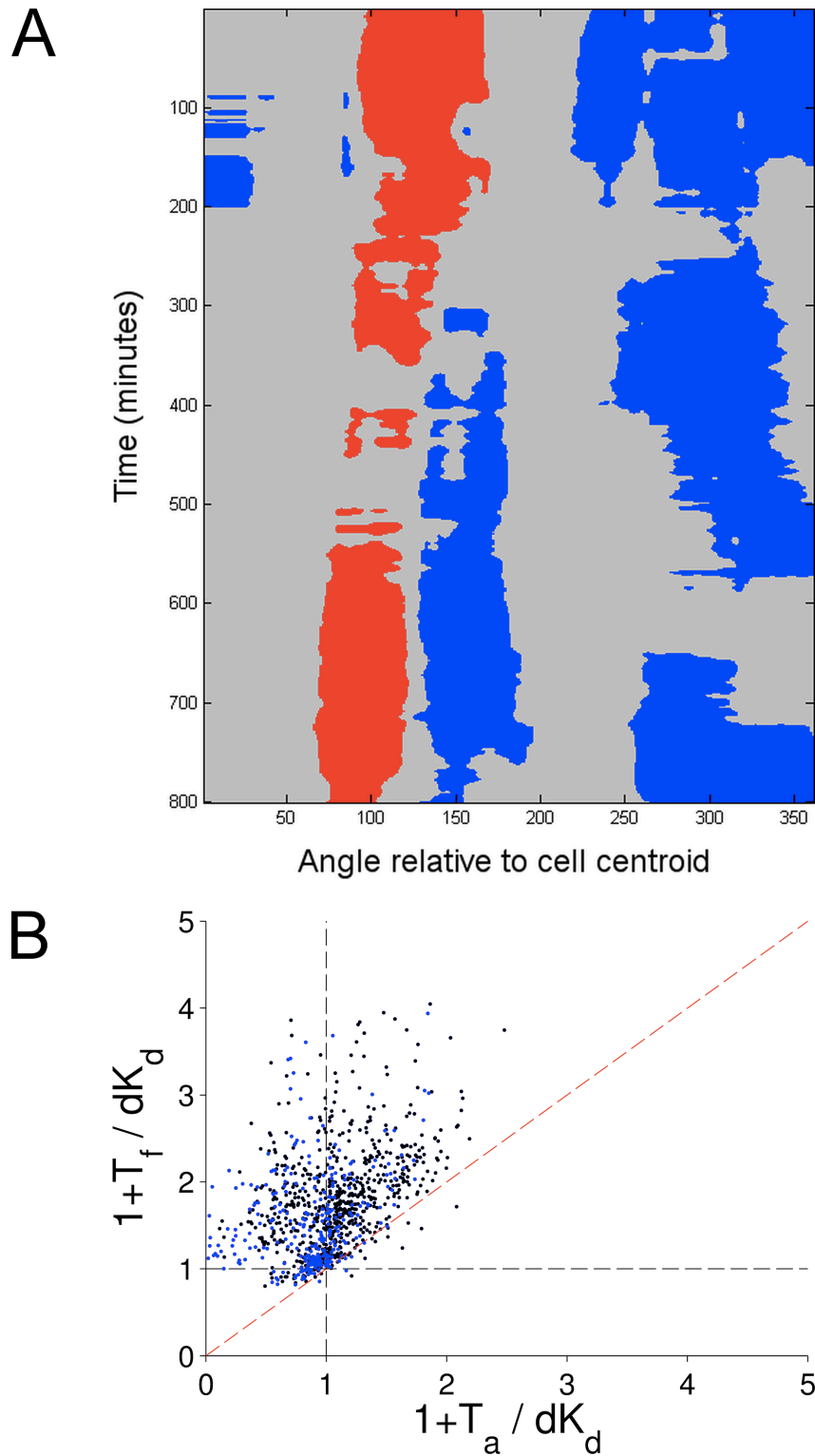


Figure S2. Classification of filopodia according to the motility status of the adjoining membrane region. a) Illustration of a representative protrusion/retraction map that was smoothed and subjected to k-means clustering. Red: protruding; gray: stationary; blue: retracting. b) Redrawing of Fig. 3D with the filopodia associated with retracting ('rear') regions marked with blue symbols and the others marked with black symbols.